

Reports

Outward-Dipping Ring-Fault Structure at Rabaul Caldera as Shown by Earthquake Locations

JIM MORI AND CHRIS MCKEE

The locations of a large number of earthquakes recorded at Rabaul caldera in Papua New Guinea from late 1983 to mid-1985 have produced a picture of this active caldera's structural boundary. The earthquake epicenters form an elliptical annulus about 10 kilometers long by 4 kilometers wide, centered in the southern part of the Rabaul volcanic complex. A set of events with well-constrained depth determinations shows a ring-fault structure that extends from the surface to a depth of about 4 kilometers and slopes steeply outward from the center of the caldera. This is the first geophysical data set that clearly outlines the orientation of an active caldera's bounding faults. This orientation, however, conflicts with the configuration of many other calderas and is not in keeping with currently preferred models of caldera formation.

THE SEISMICITY AT RABAUL CALDERA, in Papua New Guinea, greatly increased from September 1983 through July 1985. During this crisis period, monthly earthquake counts were five to ten times those of previous peak levels since recording began in 1967 (Fig. 1). The magnitudes of the earthquakes were generally quite small with one event of magnitude 5.1, seven events between magnitude 4 and 5, 56 events between magnitude 3 and 4, and tens of thousands of events of smaller magnitude. The large number of earthquakes and the increased rates of ground deformation (up to 8 cm of uplift and 60 μ rad of inflationary tilt per month) indicated the possibility of an imminent eruption (1). After 23 months the crisis period of high seismicity ended without producing an eruption; however, the large amount of earthquake data collected has allowed us to obtain a clearer picture of the subsurface structure in the caldera.

Figure 2 shows the ring pattern formed by the epicenters for more than 2500 well-constrained events during the crisis period. These locations were determined by using a version of the Fasthypo computer program (2) with a layered velocity structure determined from an explosion experiment within the caldera (3). All of the events were recorded at seven or more stations, and the horizontal uncertainties, with respect to the model, were <1 km. A similar annular pattern of seismicity was also present during the period of lower seismicity from 1977 to 1982 (1).

The recent addition of several stations to the seismic network has enabled better depth resolution for the locations presented in this report. Figure 3 shows a cross section oriented in an east-west direction through the middle of the ring pattern from 4.24°S to 4.28°S. Only events with vertical uncertainties of <1.5 km were plotted in the cross section. Seismicity trends dip steeply out-

ward; cross sections in radial directions from the northern part of the ring pattern tend to show the same trend but not as clearly, probably because of the smaller number of events. In the southern section there are too few well-constrained events to construct meaningful cross sections. The ring pattern and the outward-dipping trend of the seismicity are independent of earthquake magnitude and time (4). The large ring structure shown by the earthquake locations is interpreted to be a system of faults along which cauldron subsidence occurred at the time of the last major eruption 1400 years ago (5). During the crisis period, this zone of weakness was presumably reactivated by increased magma pressure.

Conceivably, the outward-dipping trend of the earthquakes could be a location bias due to a low-velocity region in the central part of the caldera. However, tests with a computer program to calculate the three-dimensional velocity structure (6) of the caldera showed no evidence of such a structure at shallow depth that would produce the apparent dip of the seismic zone. Earthquakes relocated by using the calculated three-dimensional velocity structure still showed the outward-dipping trend.

Observations of outward-dipping caldera faults are rare (7, 8), although Anderson (9), in a mathematical analysis of the dynamics of ring dike and cauldron subsidence formation, predicts this orientation. The appeal of Anderson's theory has long been the belief that subsidence of the roof of a magma chamber would be facilitated by outward-dipping faults and hindered or prevented by inward-dipping ones. However, geological evidence (10-12) indicates that most calderas are bounded by inward-dipping faults. These faults are presumably created in the manner of cone-sheet fractures due to compressive stresses of rising magma (13). After relaxation of magma pressure by eruption, the "space" problem of subsidence along these faults appears to be overcome by downsagging of the subsided block (10, 11). Determining the orientation of ring faults is important for interpreting the mechanics of their formation. The generation of either inward- or outward-dipping faults reflects a basic difference in the stress field that formed the faults. At Rabaul the outward-dipping faults are consistent with the Anderson model, and their formation can be associated with the stress field that was created when the roof of a large magma chamber began to lose support, probably during the course of a large-scale eruption.

Another feature of the cross section (Fig. 3) is the sharp cutoff of seismicity below 4 Rabaul Volcanological Observatory, Rabaul, Papua New Guinea.

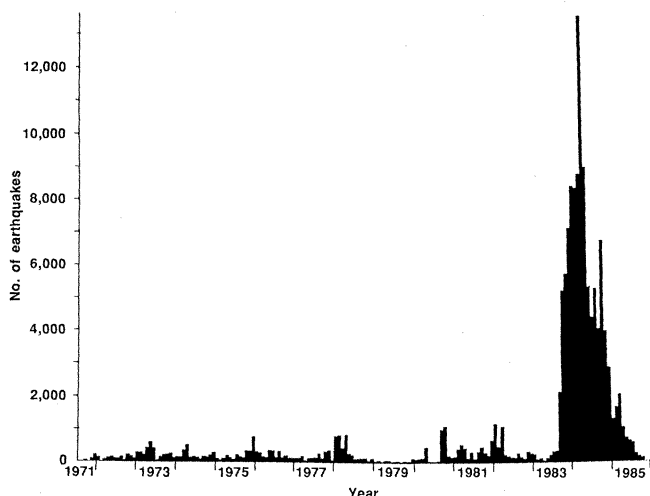


Fig. 1. Monthly earthquake totals recorded at two or more stations of the Rabaul harbor network.

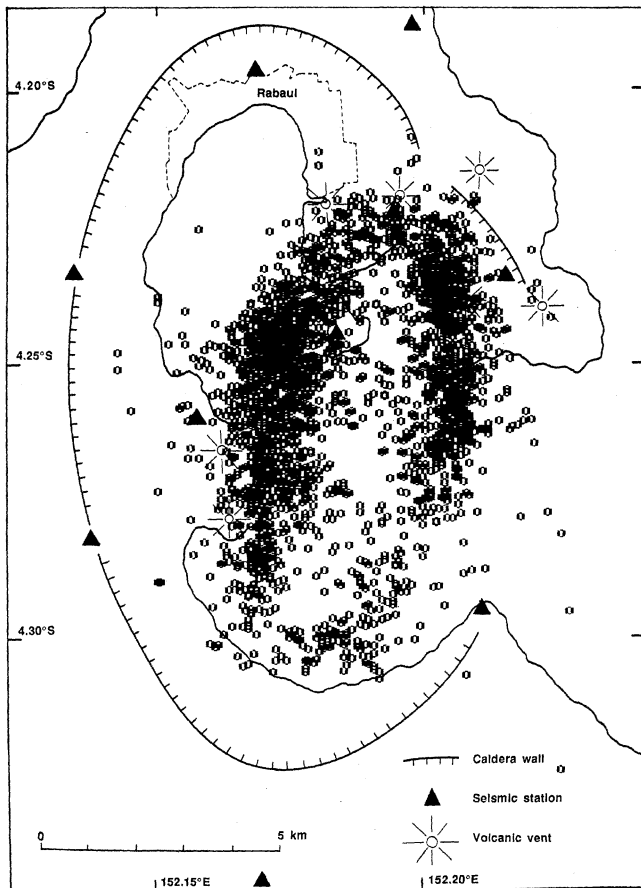
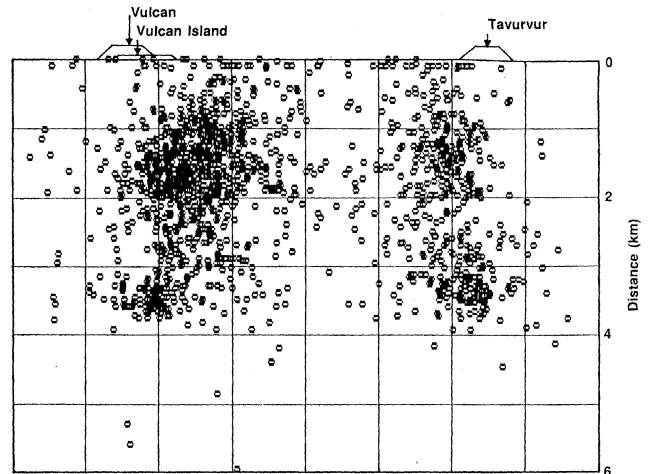


Fig. 2 (left). Epicentral locations of more than 2500 earthquakes from September 1983 through July 1985. The triangles show the positions of the ten seismic stations of the Rabaul harbor network.

Fig. 3 (below). East-west cross section through the central portion of the ring structure, showing the outward-dipping faults. Also shown are the positions of the three postcaldera vents within the region of the cross section. There is no vertical exaggeration.



km, which suggests a strong structural boundary. The termination of the fault structure at this depth indicates the extent to which brittle slip occurred along the boundary fault during the last caldera collapse. This characteristic implies that the top of the magma body active at that time was at 4 km. If the size of the magma body has not changed appreciably since the last major eruption, the top of the magma reservoir may still be at this depth.

Fault plane solutions for some of the events of larger magnitude show predominantly normal faulting (14). To be consistent with the fault orientation inferred from Fig. 3, we assumed that the outward-dipping nodal planes (which had dips of 45° to 80°) were the fault planes. This assumption implies that the region bounded by the ring structure is moving upward relative to its surroundings, which is generally consistent with the ground deformation observed during the crisis period. Measurements of ground uplift and ground tilt show substantial rise of the central part of the caldera floor (80 cm for the crisis period). However, the observed patterns indicate that most of the deformation is not caused by slip on the fault structure. The ground deformation appears to be an elastic response to one or more localized pressure sources 1 to 3 km deep within the central part of the fault-

bounded block. This interpretation is best explained by upward migration of a relatively small volume of magma from the parent body below (1).

The ring fault is not new and is almost certainly a relict of the latest caldera subsidence (1400 years ago) because outward-dipping faults would not develop in the present stress environment, which has caused updoming of the caldera floor (9, 13). Although the ring structure is a zone of weakness, it does not appear to have been intruded by magma during the recent seismo-deformational crisis. This finding is indicated by the tectonic-like character of the earthquakes and the absence of low-frequency events in the fault system. Indeed, some doubt exists that the ring fault has ever been the main channel for magma during the eruptions at the postcaldera vents, because these vents are displaced from the fault structure, at distances of about 1.0 to 1.5 km (Fig. 3). Also, the ring fault would tend to be closed by uplift of the central block during periods of increased magma pressure. The immediate source of magma for eruptions at these vents has probably been shallow magma reservoirs, such as those recently identified and located eccentrically within the caldera block. Magma may then have been channeled to the postcaldera vents along radial and cone-sheet type fractures

that developed in response to upward-directed stresses. Thus, the caldera structure would have both inward- and outward-dipping fractures, as in the model of caldera subsidence of Druitt and Sparks (15).

The striking ring pattern of seismicity, which covers a substantial portion of the caldera, indicates that stresses are distributed over a large region and are not localized near one of the individual vents. This feature may be cause for concern when considering the possibility of a future major eruption. Under the present stress regime it seems unlikely that the ring fault will be intruded by rising magma, but if the caldera block loses support from the underlying reservoir, as a result of eruption or withdrawal of magma, the ring fault would tend to open. This opening would encourage intrusion of magma into the ring fault, which could culminate in voluminous eruptions and further collapse of the caldera block. A principal concern about the next eruption will be the degree of interaction between the small shallow magma bodies and the parent reservoir below.

REFERENCES AND NOTES

1. C. O. McKee *et al.*, *Bull. Volcanol.* **47**, 397 (1984).
2. R. B. Herrmann, *Earthquake Notes* **50**, 25 (1979).
3. R. A. Almond and C. O. McKee, *Geol. Surv. Papua New Guinea, Rep.* **82-19** (1982).
4. J. Mori *et al.*, *ibid.* **86-26** (1986).

5. R. F. Heming, *Geol. Soc. Am. Bull.* **85**, 1253 (1974).
6. K. Aki and W. H. K. Lee, *J. Geophys. Res.* **81**, 4381 (1976).
7. E. B. Bailey and C. T. Clough, *Mem. Geol. Surv. Scotl.* (1924).
8. J. E. Richey and H. H. Thomas, *ibid.* (1930).
9. E. M. Anderson, *Proc. R. Soc. Edinburgh* **56**, 128 (1936).
10. D. L. Reynolds, *Verh. K. Ned. Geol. Mijnbouwk. Genoot.* **16**, 355 (1956).
11. G. P. L. Walker, *J. Geophys. Res.* **89**, 8407 (1984).
12. P. W. Lipman, *ibid.*, p. 8801.
13. W. J. Phillips, *Tectonophysics* **24**, 69 (1974).
14. J. Mori, *Int. Volcanol. Congr. N.Z.* (abstr.) (1986), p. 263.
15. T. H. Druitt and R. J. S. Sparks, *Nature (London)* **310**, 679 (1984).
16. We thank P. Lowenstein, P. de Saint Ours, and R. W. Johnson for helpful discussions and comments, J. Kuduon and C. Matupit for determining the

arrival times of the seismic events, B. Talai and I. Itikarai for work on the seismic and ground deformation data, K. Satake for help on the three-dimensional velocity inversions, and K. Shimazaki for providing the computer time. The authors publish with the permission of the secretary of the Department of Minerals and Energy, Papua New Guinea.

16 July 1986; accepted 27 October 1986

Sensory Tuning of Lateral Line Receptors in Antarctic Fish to the Movements of Planktonic Prey

JOHN C. MONTGOMERY AND JOHN A. MACDONALD

The suitability of the lateral line system of fish and aquatic amphibia for the detection of planktonic prey was examined in the antarctic fish *Pagothenia borchgrevinki* (family Nototheniidae). The best responses of primary afferent lateral line neurons to waterborne vibrations were recorded at frequencies within the range of those produced by swimming crustacea. Simultaneous recordings from a swimming zooplankter held close to the fish and from primary afferent neurons provided direct confirmation that swimming movements of crustaceans are a potent natural stimulus of the lateral line system.

THE LATERAL LINE IS AN INTERESTING and varied sensory system in fish and aquatic amphibia. The receptors of the lateral line respond to water movements (1), and the system is used in schooling (2), detection of stationary objects (3, 4), and detection of prey (5-7). However, in only a few cases can the properties of the natural stimuli be directly compared with the physiology of lateral line receptors. In this report we examine the suitability of this sensory system for the detection of planktonic prey by comparing the functional properties of the anterior lateral line system in *Pagothenia borchgrevinki* (family Nototheniidae) with the nature of the vibrations produced by the crustaceans on which it feeds. *Pagothenia borchgrevinki* is an antarctic teleost that must survive long periods of darkness during the polar winter when nonvisual systems would offer an advantage for feeding. The anterior lateral line system consists of six short dermal canals on each side of the head, opening to the outside through a series of 2 to 12 pores (Fig. 1). Vibration-sensitive neuromasts lie within the canals, one between each pair of pores.

Pagothenia borchgrevinki and zooplankton were obtained from beneath the sea ice in McMurdo Sound, Antarctica (water temperature, -1.9°C). Fish were suspended in an aquarium by a cloth sling located behind the operculum, and the gills were irrigated continuously with -1.0° to -1.5°C seawater.

Water level in the tank was adjusted to uncover the dorsal surface of the head, allowing us to make a small hole in the cranium under local anesthetic to expose the root of the anterior lateral line nerve. A vibrating sphere (4.5 mm in diameter, with a movement amplitude of 0.35 mm and a flat frequency response in the range of 1 to 90 Hz) was positioned in the water near the head of the fish while the activity of single sensory neurons was recorded from the root of the anterior lateral line nerve with glass micropipettes. Each unit responded maximally to vibration within a few millimeters of either of a contiguous pair of pores, producing one or more spikes per cycle in a

relatively constant phase relation to the stimulating sine wave. When the probe was shifted to the second pore, the phase of spikes shifted by 180° after passing through a null point; in this way each unit could be localized to a particular neuromast. The best responses were obtained with the probe in the immediate vicinity of a pore, and responses decreased as the probe was moved away from the pore, becoming barely discernible at distances of 20 to 25 mm. Most records were made from units of the mandibular and preopercular canals, which would be least subject to interference or reflections from the air-water interface.

Single units were stimulated for 30 seconds at each of a number of frequencies between 10 and 100 Hz. At low frequencies (10 to 20 Hz), units fired one to three spikes per cycle, weakly phase-locked to the stimulus cycle. At intermediate frequencies (30 to 40 Hz) the units typically fired one spike per cycle and were strongly phase-locked. At high frequencies (50 to 100 Hz), spikes were still phase-locked but occurred only every second or third stimulus cycle. We quantified the responses by determining the amplitude of spike latency histograms constructed over equal numbers of stimulus cycles for each stimulus frequency and by scaling each response as a proportion of the maximum response for the given unit. Most units responded maximally to frequencies of

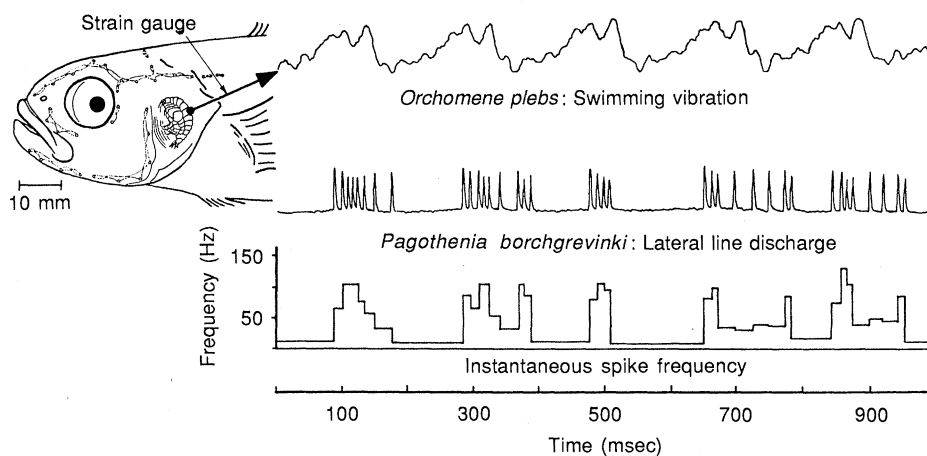


Fig. 1. Simultaneous records of the swimming vibration of an amphipod, the spike discharge of a single lateral line afferent axon (distorted in wave form owing to digitization), and its associated instantaneous spike frequency. The neuromast had previously been identified as lying between the fifth and sixth preopercular pores. The vibration record is part of the same sequence used to derive the *Orchomene plebs* power spectrum in Fig. 2B.